Please cite this article in press as: Wang et al., α-Synuclein Multimers Cluster Synaptic Vesicles and Attenuate Recycling, Current Biology (2014), http://dx.doi.org/10.1016/j.cub.2014.08.027

Current Biology *24*, 1–8, October 6, 2014 ©2014 Elsevier Ltd All rights reserved http://dx.doi.org/10.1016/j.cub.2014.08.027

Report

α-Synuclein Multimers Cluster Synaptic Vesicles and Attenuate Recycling

Lina Wang,[1,2] Utpal Das,[1,2] David A. Scott,[3] Yong Tang,[1,2,5] Pamela J. McLean,[4] and Subhojit Roy[1,2,*]

[1]Department of Pathology, University of California, San Diego, 9500 Gilman Drive, La Jolla, CA 92093, USA

[2]Department of Neurosciences, University of California, San Diego, 9500 Gilman Drive, La Jolla, CA 92093, USA

[3]McGovern Institute for Brain Research, Department of Brain and Cognitive Sciences, Department of Biological Engineering, Massachusetts Institute of Technology, Cambridge, MA 02139, USA

[4]Department of Neuroscience, Mayo Clinic, Jacksonville, FL 32224, USA

Summary

The normal functions and pathologic facets of the small presynaptic protein α-synuclein (α-syn) are of exceptional interest. In previous studies, we found that α-syn attenuates synaptic exo/endocytosis [1, 2]; however, underlying mechanisms remain unknown. More recent evidence suggests that α-syn exists as metastable multimers and not solely as a natively unfolded monomer [3–8]. However, conformations of α-syn at synapses—its physiologic locale—are unclear, and potential implications of such higher-order conformations to synaptic function are unknown. Exploring α-syn conformations and synaptic function in neurons, we found that α-syn promptly organizes into physiological multimers at synapses. Furthermore, our experiments indicate that α-syn multimers cluster synaptic vesicles and restrict their motility, suggesting a novel role for these higher-order structures. Supporting this, α-syn mutations that disrupt multimerization also fail to restrict synaptic vesicle motility or attenuate exo/endocytosis. We propose a model in which α-syn multimers cluster synaptic vesicles, restricting their trafficking and recycling, and consequently attenuate neurotransmitter release.

Results and Discussion

Contemporary Insights into α-Synuclein Biology

The presynaptic bouton is a central communicating hub, where a sequence of well-orchestrated events leads to exocytosis of neurotransmitter-loaded vesicles into the presynaptic cleft. A variety of presynaptic proteins participate, mainly assisting in the organization and trafficking of synaptic vesicles. One such protein is α-syn, which is of singular interest because of its involvement in Parkinson's disease and related movement disorders/dementias. In previous studies we found that small increments in α-syn levels lead to suppression of exo/endocytosis [1, 2] and that α-syn restricts the lateral mobility of synaptic vesicles between *en-passant* boutons [2], called "superpool" trafficking [9]. Along with other studies [10–15], available data advocate the concept that α-syn physiologically attenuates neurotransmitter release; however, underlying mechanisms are unclear. α-syn also binds to VAMP2 and promotes SNARE assembly [16], but the consequence of these interactions on synaptic physiology is uncertain [13, 16]. Regardless, a clear picture of the physiologic role of α-syn has not emerged yet.

As function often follows form in biology, understanding physiologic α-syn conformations is important. Recent studies offer surprising insights, suggesting that α-syn exists as metastable helical multimers, with predominant tetramers [3]. Though this view has been challenged [4, 5], available data from purified brain α-syn show higher-order multimers and mixed helical conformations [5, 6], consistent with the idea that α-syn exists as metastable conformers exchanging between a monomeric and multimeric state. Even so, key questions remain unresolved. What is the conformation of α-syn *at synapses*, its normal locale? Do α-syn assemblies influence its function—and if so, how? Here we couple fluorescence-complementation assays, which selectively stabilize putative α-syn assemblies, with various cell-biological paradigms to evaluate vesicle trafficking and synaptic function.

Multimeric α-Syn Conformations at Presynaptic Boutons

Though recent studies have demonstrated α-syn multimers [3, 7, 8], most experiments used biochemical or biophysical methods that do not provide spatial information; thus, α-syn conformations at the presynapse are not entirely clear. We first evaluated the organization of α-syn at synapses of cultured neurons using bimolecular fluorescence complementation (BiFC), an established method to visualize protein-protein interactions [17]. In this assay, one partner of an interacting pair is tagged to the N terminus fragment of the Venus fluorescent protein (VN), while the other partner is tagged to the complimentary C terminus (VC). If and when the two interacting partners associate, the Venus fragments are reconstituted and become fluorescent (see schematic in Figure 1Ai). Reconstitution is irreversible; thus, even transient interactions can be "captured" by these methods [18].

To mitigate concerns related to overexpression, we used a "molecular replacement strategy," where the exogenous protein is expressed in a knockout background, achieving near-physiologic expression levels [19]. Specifically, we expressed VN/VC-tagged human wild-type (WT) α-syns (VN/VC:α-syns) in cultured hippocampal neurons (days in vitro [DIV] 14) from α-syn null mice and visualized fluorescence after ~14 hr expression (strategy in Figure 1Aii). Expression of human α-syn in cultured α-syn null neurons was similar to the expression of native mouse α-syn in parallel-processed cultures (see below). Three different VN/VC-tagged α-syn combinations were used (see Supplemental Experimental Procedures available online). In all cases, robust fluorescence was seen at boutons (Figure 1B, top and Figures S1A and S1B). Cotransfection of VN and VC alone did not show any synaptic fluorescence (Figure 1B, bottom; data not shown). Complementation was also seen in nonneuronal cells as reported previously [21], and excess untagged α-syn diminished VN/VC:α-syn complementation in HEK cells, presumably by competition, suggesting

[5]Present address: Stanford University School of Medicine, 291 Campus Drive, Stanford, CA 94305, USA

*Correspondence: s1roy@ucsd.edu

Please cite this article in press as: Wang et al., α-Synuclein Multimers Cluster Synaptic Vesicles and Attenuate Recycling, Current Biology (2014), http://dx.doi.org/10.1016/j.cub.2014.08.027

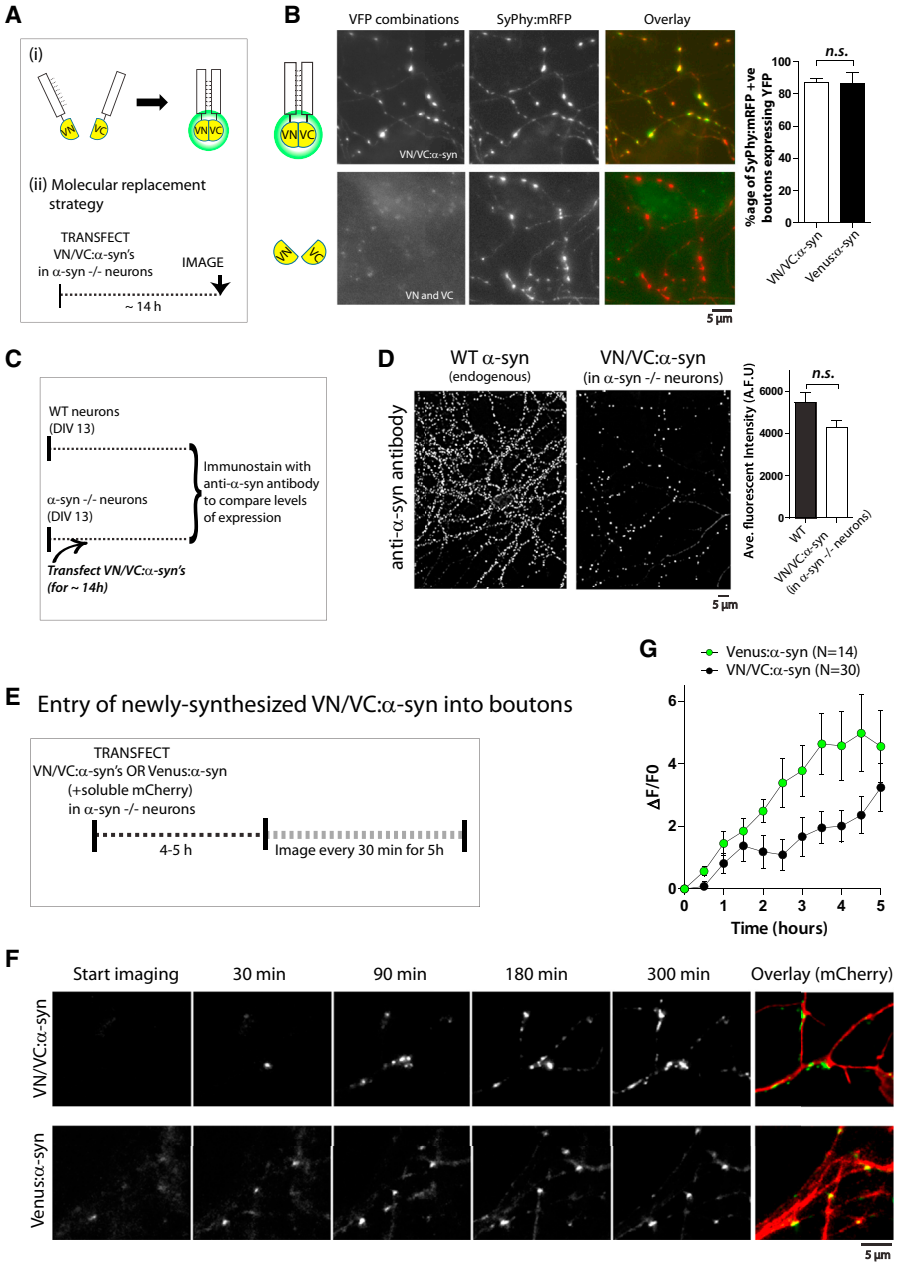

Figure 1. Multimeric α-Syn Conformations at Presynaptic Boutons

(A) Schematic of complementation assay (i) and molecular replacement strategy (ii). Cultured hippocampal neurons from α-syn −/− mice were transiently transfected with various VN/VC-tagged α-syns (see Results and Discussion) and visualized after ~14 hr.

(B) Top: representative images of reconstituted Venus fluorescence in neurons expressing VN/VC:α-syns (also see Figure S1A). Note these neurons are co-transfected with synaptophysin:mRFP (SyPhy:mRFP) to label boutons. Bottom: no fluorescence was seen in boutons expressing untagged VN + VC alone. Right: the vast majority (~85%) of SyPhy:mRFP-positive boutons also expressed VN/VC:α-syn, which is comparable to boutons expressing Venus:α-syn and SyPhy:mRFP (N ~ 700 boutons for each group from two separate batches of cultures, p = 0.90).

(C) Overall design to compare expression levels of transfected VN/VC:α-syn to endogenous mouse α-syn. Untransfected cultured neurons from WT mice and VN/VC:α-syn-transfected cultured neurons from α-syn −/− mice were fixed and immunostained with an anti-α-syn antibody (guinea pig α-syn antibody). Cell culture and immunostaining of both groups were processed in parallel. Note that while the antibody would recognize mouse α-syn in WT neurons, it would only label transfected α-syn in the VN/VC:α-syn transfected group.

(D) Representative images from the two groups in (C) (left) and quantification of overall average fluorescence intensities (right; N ~ 10 visual fields containing ~3,000–10,000 boutons; p = 0.06). Note that the number of VN/VC:α-syn transfected boutons is much lower than immunostained WT boutons (as expected with transient transfections), but the fluorescence intensities are similar.

(E) Overall design. Cultured α-syn −/− neurons were cotransfected with VN/VC:α-syns (or Venus:α-syn) + soluble mCherry, and the kinetics of initial α-syn entry and synaptic accumulation was evaluated by long-term imaging (see Results and Discussion and [20] for more details).

(F) Representative frames from two time-lapse movies showing presynaptic accumulation of VN/VC:α-syn (top) and Venus:α-syn (bottom) over 5 hr of imaging.

(G) Quantification of average VFP intensities of boutons over 5 hr. Note that although the kinetics of VN/VC:α-syn accumulation (black dots) is slower than Venus:α-syn (green dots) as expected, the difference is modest, suggesting that complementation is a relatively early event.

that complementation was specific for α-syn (Figure S1C). Synaptic fluorescence due to VN/VC:α-syn complementation was widespread and seen in virtually all transfected boutons; overall, it was similar to neurons transfected with Venus:α-syn (Figure 1B, graph on right). It is unlikely that the complementation in our experiments is an artifact of overexpression, as fluorescence intensities of transfected VN/VC:α-syn boutons in α-syn −/− neurons are similar to endogenous mouse α-syn fluorescence in WT neurons (Figures 1C and 1D; also see next paragraph).

Next we visualized the time course of accumulation of newly synthesized VN/VC:α-syn at boutons. We transfected α-syn null neurons with VN/VC:α-syn (or Venus:α-syn) and visualized the entry of newly synthesized (somatically derived) fluorescent molecules into boutons (4–5 hr after transfection), adopting an imaging strategy that we recently developed ([20], see schematic in Figure 1E). Figure 1F shows representative images from one such experiment. Note that the kinetics of VN/VC:α-syn entry into boutons is only slightly slower than Venus:α-syn, quantified in Figure 1G. These data indicate that multimerization of α-syn is an early event and likely not a consequence of abnormal long-term intramolecular associations. Also note that the experimental paradigm (visualizing entry of newly synthesized proteins into α-syn −/− boutons) further argues that the complementation is unlikely to be a result of overexpression.

α-Synuclein Multimers Cluster Synaptic Vesicles

Do α-syn multimers have a physiologic role? While qualitatively comparing the synaptic VN/VC:α-syn fluorescence with the fluorescence of endogenous or Venus:α-syn, we noticed that the reconstituted VN/VC:α-syn fluorescence seemingly occupied only a subset of the total bouton area. To verify this, we used a previously described protocol to label the entire bouton profile (using fluorescent actin, see [22]) and visualized VN/VC:α-syn fluorescence in these boutons. Indeed, reconstituted VN/VC:α-syn occupied only a fraction of the bouton area, as shown in representative bouton crops (Figure 2A). This distribution is unusual, distinct from Venus:α-syn that typically occupies the entire bouton (see Figure S2A). We also developed custom algorithms to quantify these data. Briefly, as bouton shapes vary, we measured the cross-sectional area of each bouton along 20 circumferential angles and then calculated its mean "synapse width" (see Figure 2B for general concept; see Figure S2B and Supplemental Experimental Procedures for details). Compiled data from these analyses are shown in Figures 2C and 2D. Note that the VN/VC:α-syn fluorescence only occupies a subset of the bouton cross-sectional area and is indistinguishable from the area occupied by the synaptic vesicle cluster (labeled with synaptophysin:GFP, Figure 2C). Furthermore, in neurons cotransfected with VN/VC:α-syn and synaptophysin:mRFP (SyPhy:mRFP), there is a significant overlap of fluorescence (also reflected in correlations between their "synapse widths," see Figure 2D).

Previous studies expressing WT α-syn in yeast revealed a dramatic clustering of vesicles by α-syn [23, 24]. Previously, we found that α-syn restricts synaptic vesicle motility between *en passant* boutons [2], suggesting that α-syn might cluster vesicles within synaptic boutons and restrict vesicle motility. Since α-syn multimers associate with synaptic vesicles (above), we asked whether stabilized VN/VC:α-syn multimers facilitate clustering of synaptic vesicles and inhibit vesicle motility even further. To test this, we designed an assay to directly visualize synaptic vesicle dispersion on the basis of previous observations that neuronal activity disperses synaptic vesicles from boutons into flanking axons [25, 26]. Specifically, we asked if stabilized α-syn multimers (reconstituted VN/VC:α-syns) would attenuate the activity-dependent dispersion of synaptic vesicles (labeled with SyPhy:mRFP, see Figure 2E). Indeed, while Venus:α-syn alone inhibited this dispersion (as expected), VN/VC:α-syns attenuated this dispersion even further (Figure 2F and also see Figure 4C later). Collectively, these experiments suggest that α-syn multimers associate with synaptic vesicle clusters and restrict their trafficking.

Biochemical Analysis of α-Synuclein Multimers

To biochemically evaluate α-syn multimers, we transiently introduced VN/VC:α-syns into HEK293 cells or cultured neurons (by adenoviral infections) and analyzed cell lysates by native or SDS-PAGE gels (Figure 3A). As shown in the native gels (Figure 3B), only a few higher-order α-syn bands were typically seen. Though precise molecular weights cannot be determined by these methods, these bands run at ~146 kD (α-syn tetramers would be expected to run at ~114 kD in our system: 4 α-syns + 2 VFPs). These experiments were repeated several times with similar results, and notably, all three VN/VC combinations showed similar biochemical profiles (Figure S3A).

Though our above data (Figure 2) suggest that α-syn multimers associate with synaptic vesicles, they do not directly show vesicle binding. To address this, we evaluated the association of monomeric and multimeric α-syn with purified synaptic vesicles. Based on previously published protocols [27, 28], we incubated α-syn-free synaptic vesicles and cytosol with purified monomeric or multimeric α-syn (chemically crosslinked, see [7]; Figure 3C and Figure S3B). The main advantage of this assay is that brain cytosolic factors known to affect α-syn binding to membranes are available, recapitulating the in vivo situation [27]. As shown in Figure 3D, α-syn multimers are indeed capable of binding to synaptic vesicles, though multimers are also present in cytosolic fractions. Note that these data are in general agreement with Dettmer et al., 2013.

A Mechanistic Link between α-Syn Multimerization and Synaptic Function

The above data suggest that α-syn multimers associate with and cluster synaptic vesicles. As α-syn suppresses exo/endocytosis [1, 2], one can imagine a scenario where α-syn multimers cluster synaptic vesicles, thus restricting vesicle recycling and, consequently, neurotransmitter release. If correct, this model predicts that disrupting α-syn multimers would also diminish α-syn-induced vesicle clustering and abrogate α-syn-induced synaptic attenuation. Though molecular determinants of α-syn multimerization are unknown, we reasoned that the most striking feature of the α-syn molecule—N-terminal repeats—might play a role. The N terminus of α-syn has seven 11-residue repeats that are predicted to fold into amphipathic alpha helices, highly conserved among species [29–31]. Recent simulation models also implicate these repeats in α-syn tetramerization [32]. We used a rationally designed synthetic mutant, where six threonines (T)—centrally lying along the helical face of the N terminus—are mutated to lysines (K; known as TsixK, see Figure 4A and [33]. These mutations are expected to disrupt significant portions of the extended hydrophobic face of the helix and greatly diminish the helical

Please cite this article in press as: Wang et al., α-Synuclein Multimers Cluster Synaptic Vesicles and Attenuate Recycling, Current Biology (2014), http://dx.doi.org/10.1016/j.cub.2014.08.027

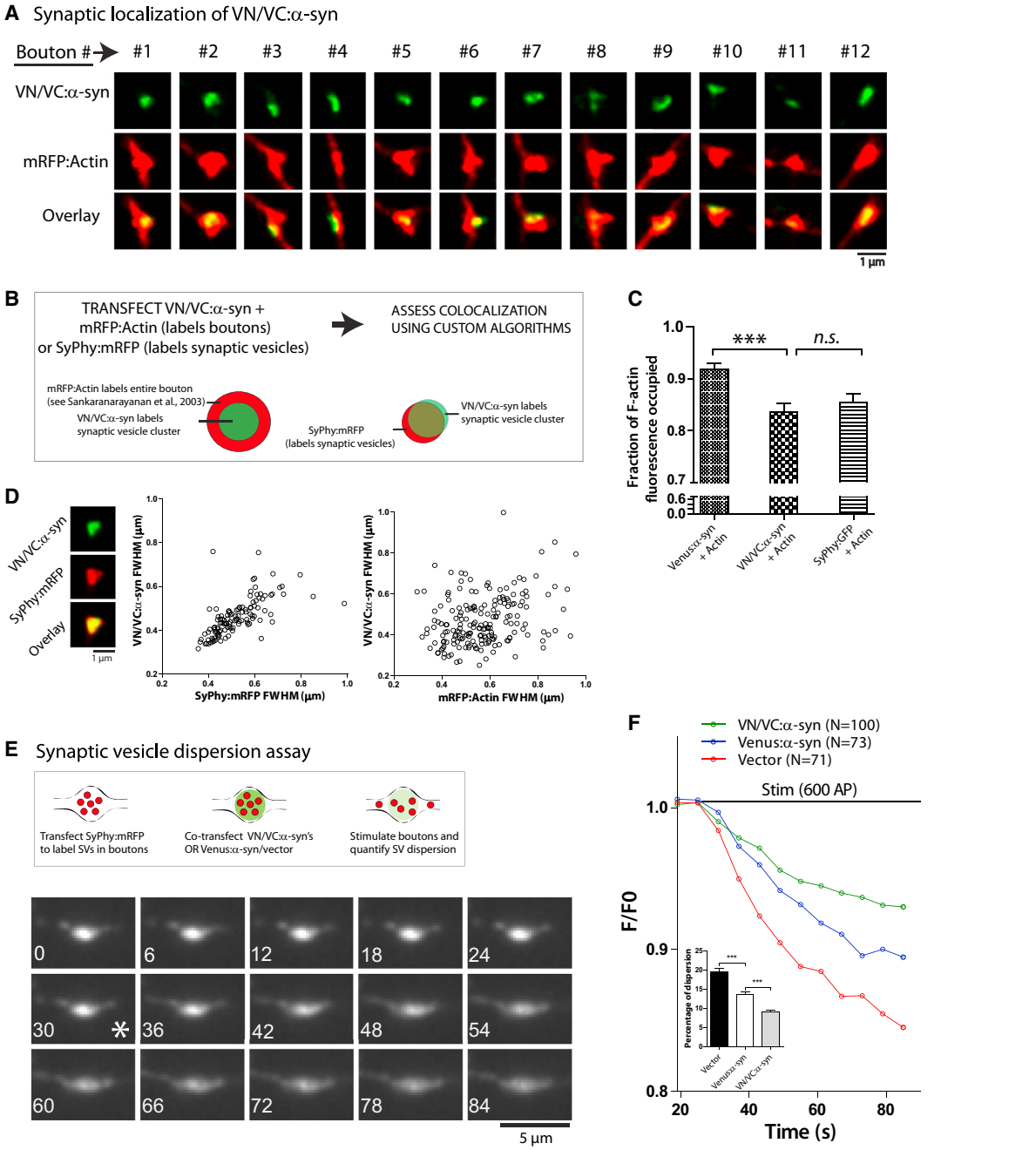

Figure 2. α-Syn Multimers Cluster Synaptic Vesicles

(A) Bouton crops from neurons cotransfected with VN/VC:α-syn and mRFP:Actin (to label the entire bouton profile, see Results and Discussion). Note that reconstituted VN/VC:α-syns only occupy a fraction of the bouton cross-sectional area.

(B) Experimental design. Neurons were cotransfected with VN/VC:α-syn and markers to label the entire bouton profile (mRFP:Actin) or synaptic vesicles (SyPhy:mRFP), and the extent of overlap was determined by custom algorithms (see Results and Discussion and Supplemental Experimental Procedures for details).

(C) Both reconstituted VN/VC:α-syn and SyPhy:GFP occupied a smaller fraction of the bouton than Venus:α-syn (~200 boutons were analyzed for each group from two separate batches of cultures, ***$p < 0.001$).

(D) Bouton widths (full-width half-max, see Supplemental Experimental Procedures) of VN/VC:α-syn and SyPhy:mRFP were correlated (left; $r = 0.36$, $p < 0.0001$), unlike VN/VC:α-syn and mRFP:Actin (right), further indicating associations of complemented VN/VC:α-syns with synaptic vesicles (N = 120 boutons from two separate batches of cultures).

(E) Top: schematic of "synaptic vesicle dispersion assay." Synaptic vesicles are labeled by SyPhy:mRFP, and neurons are stimulated to disperse synaptic vesicles (see Results and Discussion). Bottom: a time-series showing dispersion of synaptic vesicles from a bouton (elapsed time is in seconds on the lower left, and the asterisk marks the start of stimulation).

(F) Quantification of synaptic vesicle dispersion using above assay. While Venus:α-syn diminishes dispersion kinetics (compared with vector), the dispersion is further attenuated by VN/VC:α-syn (note that error bars are too small to be seen). The extent of the dispersion is quantified in the inset (19.5%, 13.6%, and 9% of total synaptic vesicles were dispersed in vector, Venus:α-syn, and VN/VC:α-syn groups, respectively; ***$p < 0.001$, unpaired t test).

Please cite this article in press as: Wang et al., α-Synuclein Multimers Cluster Synaptic Vesicles and Attenuate Recycling, Current Biology (2014), http://dx.doi.org/10.1016/j.cub.2014.08.027

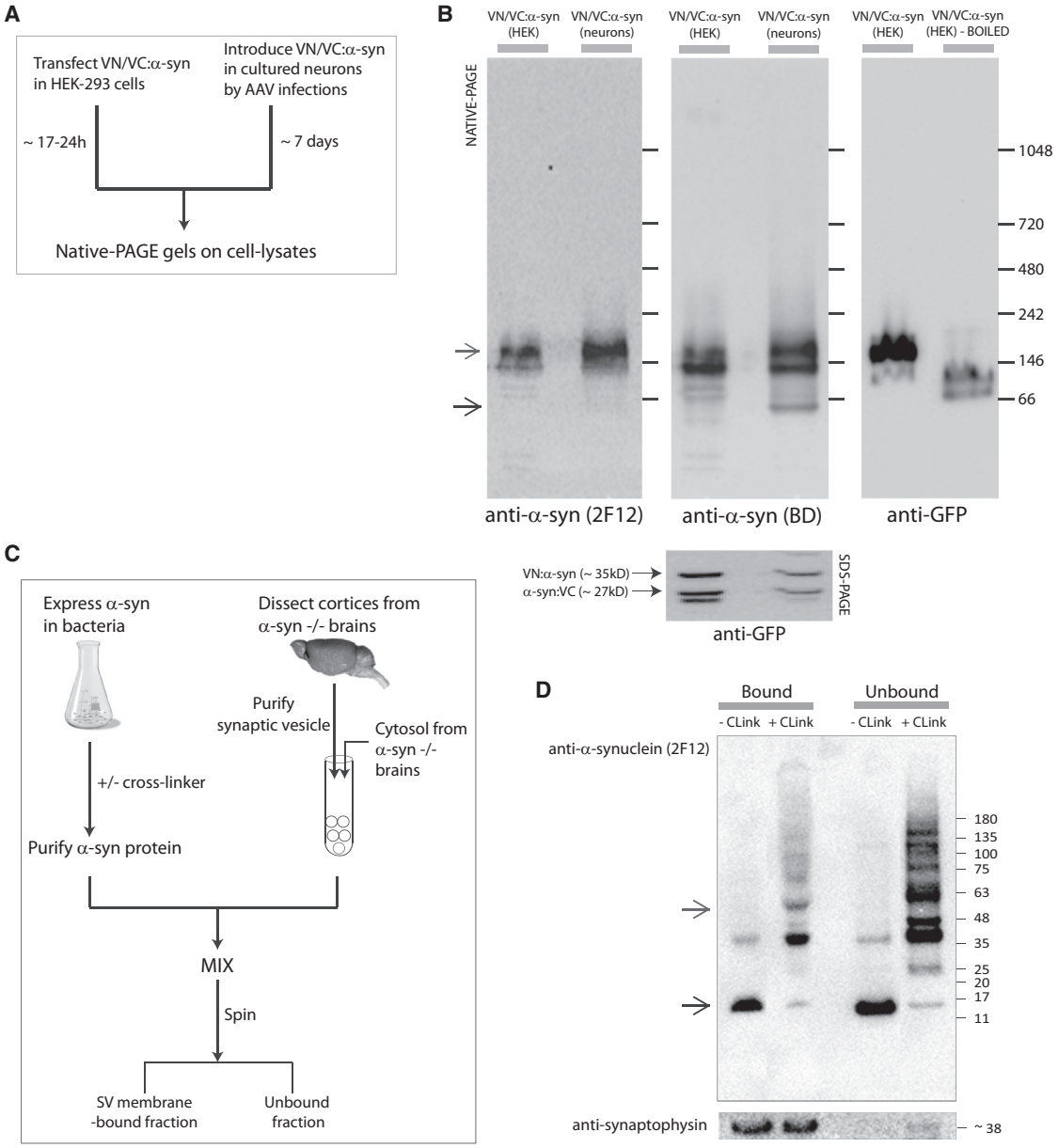

Figure 3. Biochemical Analyses of α-Syn Multimers

(A) VN/VC:α-syns were introduced into HEK293T cells or neurons (by viruses) and expressed for the times indicated, and cell lysates were analyzed by native or SDS-PAGE.

(B) Native-PAGE show α-syn higher-order multimers immunoblotted with two α-syn antibodies and an anti-GFP antibody that also recognizes YFP (note disruption upon boiling). The top arrow marks the position where bands are typically seen, and the bottom arrow marks putative monomeric α-syn in neurons. An SDS-PAGE immunoblotted with anti-GFP marks the VFP fragments. Each experiment was repeated 3–5 times with similar results.

(C) In vitro reconstitution assay. Purified synaptic vesicles and cytosol from α-syn −/− mouse brains were mixed with WT-α-syn purified from bacteria with/without a chemical cross linker (DSG). Vesicle membrane bound and unbound fractions were separated by centrifugation and analyzed by SDS-PAGE.

(D) Both monomeric and crosslinked α-syn multimers bound to synaptic vesicles (a synaptophysin stain confirms that all synaptic vesicles are in the bound fraction). Top and bottom arrows mark positions of putative tetramers and monomers. The experiment was repeated twice with similar results.

conformation of α-syn [33]. Notably, this reduction in helicity occurs despite robust association with vesicles [33], and indeed both WT and TsixK protein bind synaptic vesicles with equal affinity in our in vitro assay (Figure S3C).

Accordingly, we tested the predictions of our model by comparing the ability of WT and TsixK mutants to (1) organize into multimers, (2) cluster synaptic vesicles, and (3) influence synaptic vesicle recycling. First, we transfected VN/VC pairs of WT α-syns (VN/VC:WT) or TsixK α-syns (VN/VC:TsixK) in cultured neurons from α-syn −/− mice as described previously. As shown in Figure 4B, fluorescence complementation in the VN/VC:TsixK α-syns was markedly attenuated. Diminution of higher-order conformers was also seen biochemically (Figure S3D). Next, we tested the ability of the TsixK mutant to suppress activity-induced synaptic vesicle dispersion. As shown in Figure 4C, while WT α-syn attenuated synaptic

Please cite this article in press as: Wang et al., α-Synuclein Multimers Cluster Synaptic Vesicles and Attenuate Recycling, Current Biology (2014), http://dx.doi.org/10.1016/j.cub.2014.08.027

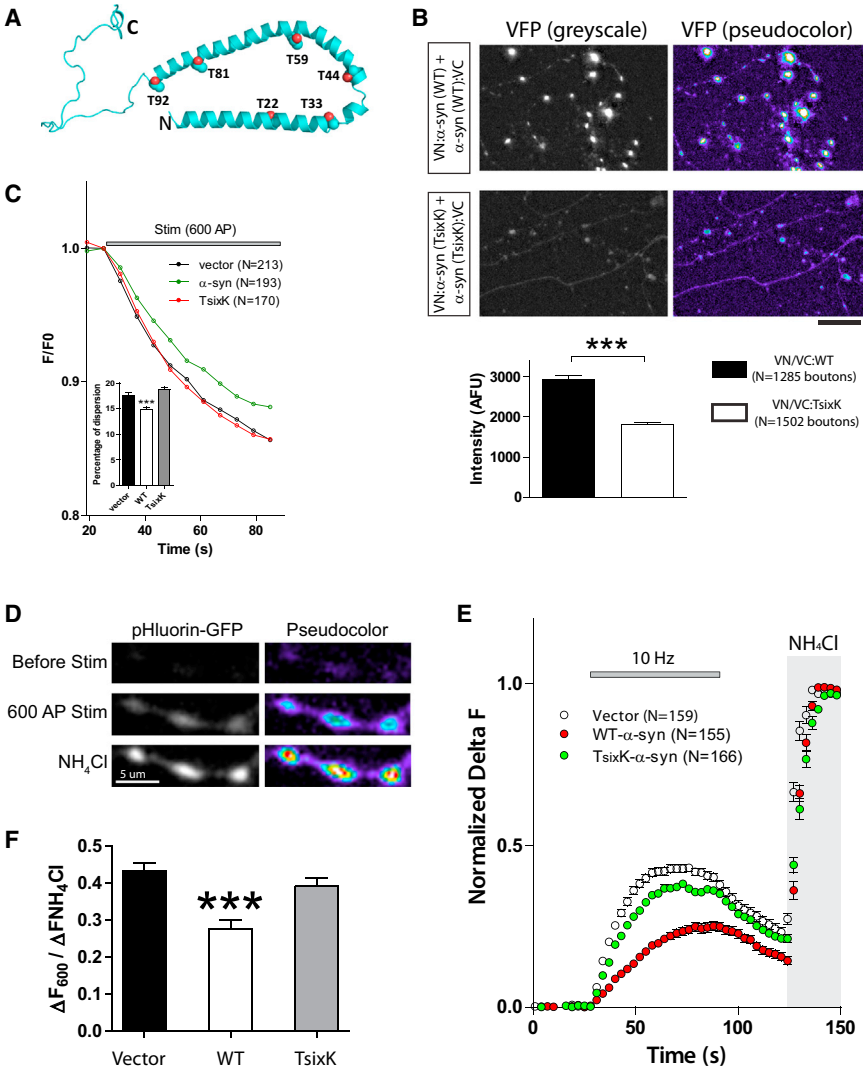

Figure 4. Mechanistic Links between α-Syn Multimerization and Synaptic Function

(A) Schematic of the α-syn helices (shaded) and position of the six mutations.

(B) Neurons from α-syn −/− mice were transfected with VN/VC:WT or VN/VC:TsixK α-syns, and fluorescence was quantified in boutons. Scale bar represents 5 μm. There were clear diminutions in the TsixK data sets as shown in the representative images and quantification below.

(C) "Synaptic vesicle dispersion" assay. Neurons were cotransfected with SyPhy:mRFP (to label synaptic vesicles) and untagged WT or TsixK α-syn (or vector alone). Boutons were stimulated and decay of RFP fluorescence from boutons was quantified (see Results and Discussion). Note that while WT α-syn attenuates activity-induced synaptic vesicle dispersion, the TsixK mutant has no effect on vesicle trafficking (N = number of boutons).

(D) Synaptic recycling evaluated by vGlut-pHluorin assays. Cultured neurons were cotransfected with vGlut-pHluorin and either untagged WT α-syn or TsixK α-syn. The fluorescence change of the pH-sensitive vGlut-pHluorin probe reflects synaptic vesicle recycling in this assay (see Results, Discussion, and Supplemental Experimental Procedures). Representative panels show the fluorescence intensity change of vGlut-pHluorin upon 600 AP stimulation and NH_4Cl perfusion. Note that NH_4Cl alkalinizes all vesicles, revealing the total (recycling + resting) pool in these neurons.

(E) Representative ensemble average of vGlut-pHluorin traces from empty vector, WT α-syn, or TsixK α-syn transfected neurons (N = number of boutons). Note that while WT α-syn attenuates neurotransmitter release and decreases mean recycling pools compared with vector controls, TsixK α-syn fails to show this effect and is quantified in (F) (all data normalized to total pools).

(F) Recycling:total pool ratio for vector = 43% ± 2.17%; WT α-syn = 28% ± 2.38%; and TsixK α-syn = 39% ± 2.29% (~160 boutons on 7–9 coverslips were analyzed for each group from three separate batches of cultures; ***$p < 0.001$ compared with vector by one-way ANOVA followed by Dunnet's post hoc test). Total (alkalinized) pools of vector, WT-α-syn, and TsixK-α-syn groups were 317.1 ± 16 arbitrary fluorescence units (AFU), 317.5 ± 11 AFU, and 376 ± 18 AFU (mean ± SEM), respectively.

vesicle dispersion as expected, the TsixK mutant failed to do so. Finally, to find whether TsixK mutations also abrogated the ability of α-syn to attenuate synaptic vesicle recycling, we used a phluorin-based assay that directly reports synaptic vesicle recycling ([34, 35]; see Figure 4D). While WT-α-syn attenuated recycling as reported previously [11], TsixK-α-syn only had a mild (nonsignificant) effect (Figures 4E and 4F).

Dynamic α-Synuclein Multimers at Synapses

Collectively, the data support a model where synaptic α-syn is organized into metastable conformers that bind to and cluster synaptic vesicles, restricting their trafficking. We posit that by influencing synaptic vesicle trafficking, multimeric α-syn conformers restrict recycling, consequently attenuating neurotransmitter release. Using complementation assays that stabilize putative protein-protein interactions, we found that near-physiologic levels of α-syn result in robust and widespread complementation at synapses (Figure 1). Given the transient transfection of proteins into an α-syn null background, the resultant low expression levels (comparable to endogenous levels, see Figure 1D), and the paradigms used to visualize initial entry of newly synthesized α-syn into boutons (Figures 1E–1G), it is unlikely that the complementation seen in our experiments is a result of overexpression. Moreover, data from three different combinations of VN/VC fragments (tagged to α-syns) are similar, untagged α-syn appears to compete with fluorescence complementation in HEK cells, and the TsixK α-syn mutant also fails to complement, collectively arguing that complementation is not due to vagaries of the Venus fragments, but reflect bona fide α-syn interactions.

Clustering Synaptic Vesicles and Regulating Recycling/Neurotransmitter Release: A Potential Function of α-Syn Multimers

Do α-syn multimers have a physiologic role? Stabilized VN/VC:α-syn multimers were associated with synaptic vesicles (Figures 2A–2D), and also inhibited the trafficking of synaptic vesicles (Figures 2E and 2F and also Figure 4C). Our biochemical data also show that α-syn multimers can associate with synaptic vesicles (Figure 3D). Notably, the data do not rule out a role for cytosolic α-syn multimers. A recent study showed that purified α-syn protein clusters synthetic vesicles in an

in vitro lipid-binding assay [36]. Though in isolation, the relevance of these purely in vitro findings to neurons and synapses is uncertain; in light of data shown here, the collective evidence advocate the concept that α-syn plays a physiologic role in clustering synaptic vesicles. Supporting the idea that helical folding of α-syn is important for multimerization, Varkey et al. recently showed that incubation of α-syn with lipid nanoparticles—known to induce helicity—increases intramolecular fluorescence resonance energy transfer of α-syn [37]. However, another recent paper suggests that α-syn is exclusively involved in attenuating endocytosis [38]. Nevertheless, many studies indicate that α-syn influences the exocytic cycle and SNARE assemblies, and a more complete dissection of exocytosis versus endocytosis is warranted. The exact mechanisms by which α-syn multimers restrict vesicle mobility are still unclear. One possibility is that α-syn multimers between adjacent vesicles associate with each other (an "interlocking model"), with perhaps α-syn/VAMP2 interactions also playing a role, which is an open question for future studies.

Supplemental Information

Supplemental Information includes Supplemental Experimental Procedures and three figures and can be found with this article online at http://dx.doi.org/10.1016/j.cub.2014.08.027.

Acknowledgments

We thank Julia George (University of London) for the original TsixK plasmid; Shelley Halpain and Barbara Calabrese (UCSD) for the mRFP:Actin construct; Timothy Ryan (Weill Cornell) for pHluorin constructs and technical advice; and Tim Bartels and Dennis Selkoe (Harvard) for the 2F12 antibody. We also thank Virginia Lee (University of Pennsylvania), Leon Laganado (MRC, Cambridge), and Christoph Kaether (Leibniz Institute, Jena) for the guinea pig synuclein antibody, synaptophysin:mRFP, and synaptophysin:GFP constructs, respectively. This work was supported by grants to S.R. (P50AG005131—project 2, NIH) and P.J.M. (RO1 NS073740, NIH).

Received: July 5, 2014
Revised: August 1, 2014
Accepted: August 13, 2014
Published: September 25, 2014

References

1. Scott, D.A., Tabarean, I., Tang, Y., Cartier, A., Masliah, E., and Roy, S. (2010). A pathologic cascade leading to synaptic dysfunction in alpha-synuclein-induced neurodegeneration. J. Neurosci. *30*, 8083–8095.
2. Scott, D., and Roy, S. (2012). α-Synuclein inhibits intersynaptic vesicle mobility and maintains recycling-pool homeostasis. J. Neurosci. *32*, 10129–10135.
3. Bartels, T., Choi, J.G., and Selkoe, D.J. (2011). α-Synuclein occurs physiologically as a helically folded tetramer that resists aggregation. Nature *477*, 107–110.
4. Fauvet, B., Mbefo, M.K., Fares, M.B., Desobry, C., Michael, S., Ardah, M.T., Tsika, E., Coune, P., Prudent, M., Lion, N., et al. (2012). α-Synuclein in central nervous system and from erythrocytes, mammalian cells, and *Escherichia coli* exists predominantly as disordered monomer. J. Biol. Chem. *287*, 15345–15364.
5. Burré, J., Vivona, S., Diao, J., Sharma, M., Brunger, A.T., and Sudhof, T.C. (2013). Properties of native brain α-synuclein. Nature *498*, E4–E6.
6. Gould, N., Mor, D.E., Lightfoot, R., Malkus, K., Giasson, B., and Ischiropoulos, H. (2014). Evidence of native α-synuclein conformers in the human brain. J. Biol. Chem. *289*, 7929–7934.
7. Dettmer, U., Newman, A.J., Luth, E.S., Bartels, T., and Selkoe, D. (2013). In vivo cross-linking reveals principally oligomeric forms of α-synuclein and β-synuclein in neurons and non-neural cells. J. Biol. Chem. *288*, 6371–6385.
8. Wang, W., Perovic, I., Chittuluru, J., Kaganovich, A., Nguyen, L.T., Liao, J., Auclair, J.R., Johnson, D., Landeru, A., Simorellis, A.K., et al. (2011). A soluble α-synuclein construct forms a dynamic tetramer. Proc. Natl. Acad. Sci. USA *108*, 17797–17802.
9. Staras, K., Branco, T., Burden, J.J., Pozo, K., Darcy, K., Marra, V., Ratnayaka, A., and Goda, Y. (2010). A vesicle superpool spans multiple presynaptic terminals in hippocampal neurons. Neuron *66*, 37–44.
10. Larsen, K.E., Schmitz, Y., Troyer, M.D., Mosharov, E., Dietrich, P., Quazi, A.Z., Savalle, M., Nemani, V., Chaudhry, F.A., Edwards, R.H., et al. (2006). Alpha-synuclein overexpression in PC12 and chromaffin cells impairs catecholamine release by interfering with a late step in exocytosis. J. Neurosci. *26*, 11915–11922.
11. Nemani, V.M., Lu, W., Berge, V., Nakamura, K., Onoa, B., Lee, M.K., Chaudhry, F.A., Nicoll, R.A., and Edwards, R.H. (2010). Increased expression of alpha-synuclein reduces neurotransmitter release by inhibiting synaptic vesicle reclustering after endocytosis. Neuron *65*, 66–79.
12. Lundblad, M., Decressac, M., Mattsson, B., and Björklund, A. (2012). Impaired neurotransmission caused by overexpression of α-synuclein in nigral dopamine neurons. Proc. Natl. Acad. Sci. USA *109*, 3213–3219.
13. Greten-Harrison, B., Polydoro, M., Morimoto-Tomita, M., Diao, L., Williams, A.M., Nie, E.H., Makani, S., Tian, N., Castillo, P.E., Buchman, V.L., and Chandra, S.S. (2010). αβγ-Synuclein triple knockout mice reveal age-dependent neuronal dysfunction. Proc. Natl. Acad. Sci. USA *107*, 19573–19578.
14. Anwar, S., Peters, O., Millership, S., Ninkina, N., Doig, N., Connor-Robson, N., Threlfell, S., Kooner, G., Deacon, R.M., Bannerman, D.M., et al. (2011). Functional alterations to the nigrostriatal system in mice lacking all three members of the synuclein family. J. Neurosci. *31*, 7264–7274.
15. Abeliovich, A., Schmitz, Y., Fariñas, I., Choi-Lundberg, D., Ho, W.H., Castillo, P.E., Shinsky, N., Verdugo, J.M., Armanini, M., Ryan, A., et al. (2000). Mice lacking alpha-synuclein display functional deficits in the nigrostriatal dopamine system. Neuron *25*, 239–252.
16. Burré, J., Sharma, M., Tsetsenis, T., Buchman, V., Etherton, M.R., and Südhof, T.C. (2010). Alpha-synuclein promotes SNARE-complex assembly in vivo and in vitro. Science *329*, 1663–1667.
17. Kerppola, T.K. (2006). Design and implementation of bimolecular fluorescence complementation (BiFC) assays for the visualization of protein interactions in living cells. Nat. Protoc. *1*, 1278–1286.
18. Kodama, Y., and Hu, C.D. (2012). Bimolecular fluorescence complementation (BiFC): a 5-year update and future perspectives. Biotechniques *53*, 285–298.
19. Schlüter, O.M., Xu, W., and Malenka, R.C. (2006). Alternative N-terminal domains of PSD-95 and SAP97 govern activity-dependent regulation of synaptic AMPA receptor function. Neuron *51*, 99–111.
20. Tang, Y., Scott, D., Das, U., Gitler, D., Ganguly, A., and Roy, S. (2013). Fast vesicle transport is required for the slow axonal transport of synapsin. J. Neurosci. *33*, 15362–15375.
21. Outeiro, T.F., Putcha, P., Tetzlaff, J.E., Spoelgen, R., Koker, M., Carvalho, F., Hyman, B.T., and McLean, P.J. (2008). Formation of toxic oligomeric alpha-synuclein species in living cells. PLoS One *3*, e1867.
22. Sankaranarayanan, S., Atluri, P.P., and Ryan, T.A. (2003). Actin has a molecular scaffolding, not propulsive, role in presynaptic function. Nat. Neurosci. *6*, 127–135.
23. Soper, J.H., Roy, S., Stieber, A., Lee, E., Wilson, R.B., Trojanowski, J.Q., Burd, C.G., and Lee, V.M. (2008). Alpha-synuclein-induced aggregation of cytoplasmic vesicles in *Saccharomyces cerevisiae*. Mol. Biol. Cell *19*, 1093–1103.
24. Gitler, A.D., Bevis, B.J., Shorter, J., Strathearn, K.E., Hamamichi, S., Su, L.J., Caldwell, K.A., Caldwell, G.A., Rochet, J.C., McCaffery, J.M., et al. (2008). The Parkinson's disease protein alpha-synuclein disrupts cellular Rab homeostasis. Proc. Natl. Acad. Sci. USA *105*, 145–150.
25. Fortin, D.L., Nemani, V.M., Voglmaier, S.M., Anthony, M.D., Ryan, T.A., and Edwards, R.H. (2005). Neural activity controls the synaptic accumulation of alpha-synuclein. J. Neurosci. *25*, 10913–10921.
26. Sankaranarayanan, S., and Ryan, T.A. (2000). Real-time measurements of vesicle-SNARE recycling in synapses of the central nervous system. Nat. Cell Biol. *2*, 197–204.
27. Wislet-Gendebien, S., D'Souza, C., Kawarai, T., St George-Hyslop, P., Westaway, D., Fraser, P., and Tandon, A. (2006). Cytosolic proteins regulate alpha-synuclein dissociation from presynaptic membranes. J. Biol. Chem. *281*, 32148–32155.

28. Wislet-Gendebien, S., Visanji, N.P., Whitehead, S.N., Marsilio, D., Hou, W., Figeys, D., Fraser, P.E., Bennett, S.A., and Tandon, A. (2008). Differential regulation of wild-type and mutant alpha-synuclein binding to synaptic membranes by cytosolic factors. BMC Neurosci. *9*, 92.
29. Davidson, W.S., Jonas, A., Clayton, D.F., and George, J.M. (1998). Stabilization of alpha-synuclein secondary structure upon binding to synthetic membranes. J. Biol. Chem. *273*, 9443–9449.
30. Jo, E., McLaurin, J., Yip, C.M., St George-Hyslop, P., and Fraser, P.E. (2000). alpha-Synuclein membrane interactions and lipid specificity. J. Biol. Chem. *275*, 34328–34334.
31. Ulmer, T.S., and Bax, A. (2005). Comparison of structure and dynamics of micelle-bound human alpha-synuclein and Parkinson disease variants. J. Biol. Chem. *280*, 43179–43187.
32. Kara, E., Lewis, P.A., Ling, H., Proukakis, C., Houlden, H., and Hardy, J. (2013). α-Synuclein mutations cluster around a putative protein loop. Neurosci. Lett. *546*, 67–70.
33. Perrin, R.J., Woods, W.S., Clayton, D.F., and George, J.M. (2000). Interaction of human alpha-synuclein and Parkinson's disease variants with phospholipids. Structural analysis using site-directed mutagenesis. J. Biol. Chem. *275*, 34393–34398.
34. Burrone, J., Li, Z., and Murthy, V.N. (2006). Studying vesicle cycling in presynaptic terminals using the genetically encoded probe synaptopHluorin. Nat. Protoc. *1*, 2970–2978.
35. Balaji, J., and Ryan, T.A. (2007). Single-vesicle imaging reveals that synaptic vesicle exocytosis and endocytosis are coupled by a single stochastic mode. Proc. Natl. Acad. Sci. USA *104*, 20576–20581.
36. Diao, J., Burré, J., Vivona, S., Cipriano, D.J., Sharma, M., Kyoung, M., Südhof, T.C., and Brunger, A.T. (2013). Native α-synuclein induces clustering of synaptic-vesicle mimics via binding to phospholipids and synaptobrevin-2/VAMP2. eLife *2*, e00592.
37. Varkey, J., Mizuno, N., Hegde, B.G., Cheng, N., Steven, A.C., and Langen, R. (2013). α-Synuclein oligomers with broken helical conformation form lipoprotein nanoparticles. J. Biol. Chem. *288*, 17620–17630.
38. Vargas, K.J., Makani, S., Davis, T., Westphal, C.H., Castillo, P.E., and Chandra, S.S. (2014). Synucleins regulate the kinetics of synaptic vesicle endocytosis. J. Neurosci. *34*, 9364–9376.

Current Biology, Volume *24*

Supplemental Information

α-Synuclein Multimers Cluster Synaptic Vesicles and Attenuate Recycling

Lina Wang, Utpal Das, David A. Scott, Yong Tang, Pamela J. McLean, and Subhojit Roy

SUPPLEMENTARY FIGURES

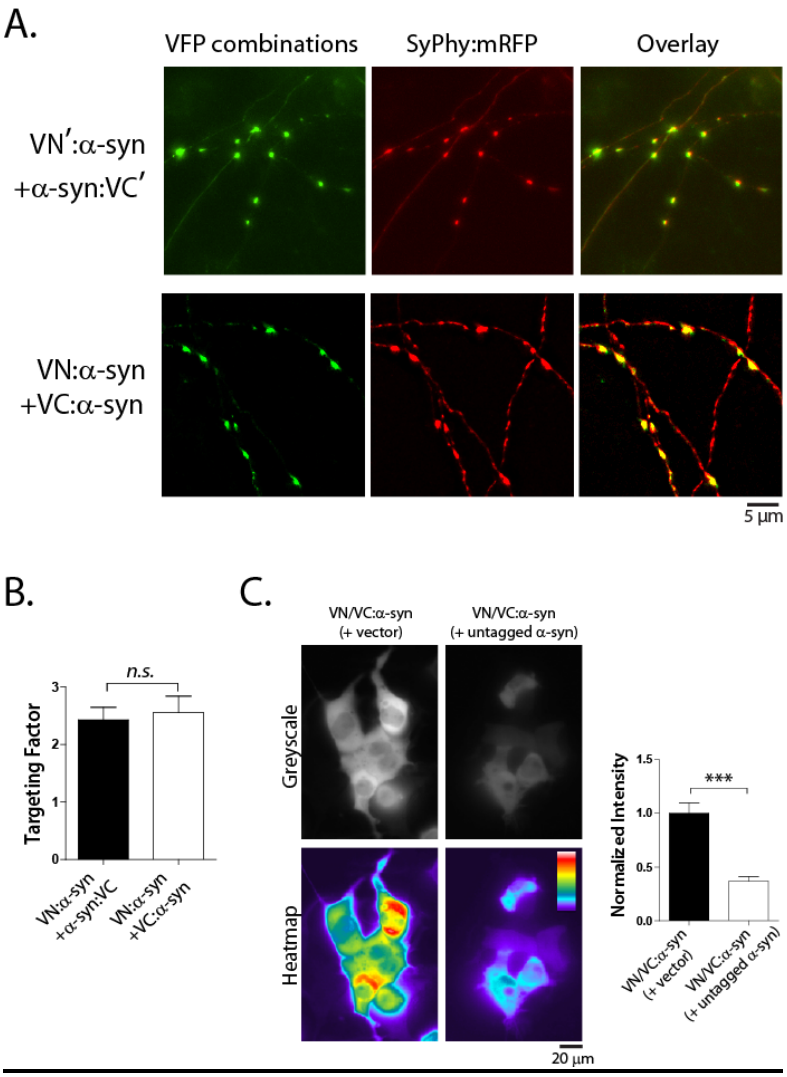

<u>Supplementary figure S1</u>: [Related to figure 1]

(A) Two other VN/VC combinations (marked VN', VC', see "methods" for sequence details) also show widespread and robust synaptic fluorescence. Cultured neurons (~ DIV-14) were co-transfected with VN/VC α-syn's and SyPhy:mRFP and imaged live; representative images are shown.

(B) Targeting factors (see "methods") of different VN/VC-tagged α-syn's were similar (p=0.77; unpaired t test).

(C) HEK-293 cells were transfected with either VN/VC:α-syn's + empty vector, or VN/VC:α-syn's + untagged α-syn. Fluorescence-intensities in the latter group was visibly lower, quantified on right (N~ 50 cells analyzed for each group).

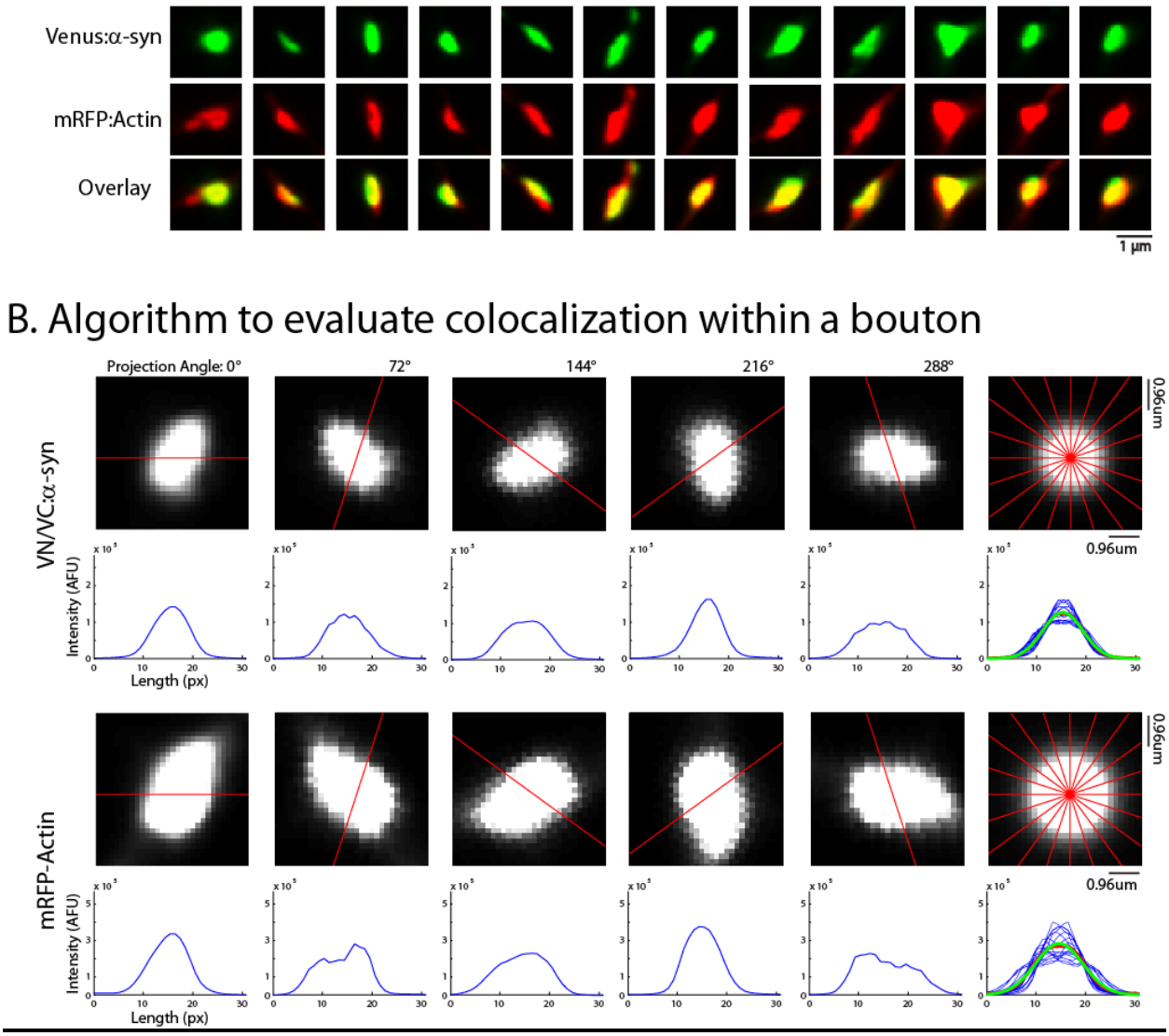

Supplementary figure S2: [Related to figure 2]

(A) Bouton-crops from neurons transfected with Venus:α-syn and mRFP:Actin (to label entire bouton). Note that the Venus α-syn fluorescence occupies the entire bouton-area, unlike VN/VC:α-syn's (compare with fig. 2A).

(B) Illustrative examples of custom algorithm to evaluate synapse-widths. Data from a single bouton expressing VN/VC:α-syn (top) and mRFP:Actin (bottom) is shown. For each bouton, the algorithm generated linescans at 20 circumferential angles around a weighted centroid (only 5 such angles are shown for clarity). For each linescan, linear fluorescence projections were obtained. Finally, mean of the 20 resultant line scans was approximated with a first order Gaussian, and the synaptic width (FWHM, see "methods") was calculated from these data. Frame on extreme right shows the synthetic data from the algorithms with the overlaid linescans.

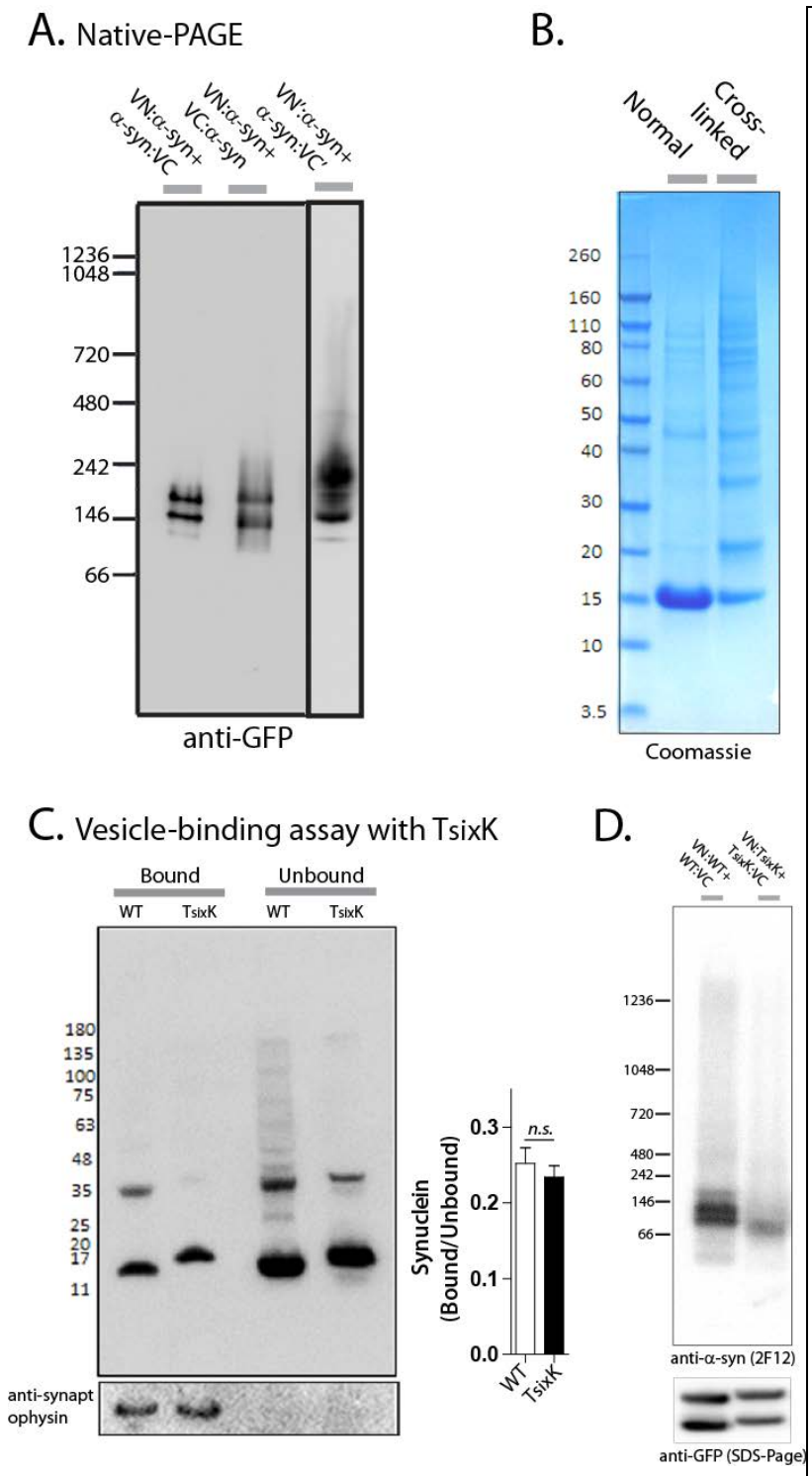

Supplementary figure S3:
[Related to figure 3]

(A) Native-PAGE gels from all VN/VC:α-syn combinations are similar. HEK-293T cells were transfected with VN:α-syn + α-syn:VC; VN:α-syn + VC:α-syn, or VN':α-syn + α-syn:VC'. After ~ 24h, cells were lysed, run on a Native-PAGE gel and immunoblotted with an anti-GFP antibody.

(B) WT-α-syn expressed and purified from bacteria (Coomassie). A major ~ 15kD band is seen as expected, as well as a minor band corresponding to dimers (also see [S1]. Note increase in high molecular-weight bands upon cross-linking.)

(C) Purified WT or TsixK α-syn protein was incubated with synaptic vesicles/cytosol as described in the "results" and "methods". Note that relative amounts of protein bound to synaptic vesicles were similar in both groups.

(D) HEK293T cells were transfected with VN/VC:WT-α-syn or VN/VC:TsixK-α-syn and lysates were analyzed by Native-PAGE after ~ 24h. Note that the TsixK mutations attenuate higher-order multimers (GFP-staining of SDS-treated samples confirm equivalent loading). Experiments were repeated five times with similar results.

SUPPLEMENTAL EXPERIMENTAL PROCEDURES

DNA Constructs and antibodies

VN/VC constructs were as follows. 1) VN:α-syn + α-syn:VC: VN (1-158)-IDGGGGSGGGGSLK-α-syn and α-syn-LE-VC (159-239) [S2]; (2) VN':α-syn + α-syn:VC': VN (1-172)-QAS-α-syn and α-syn-PRARDPPVAT-VC (155-238) [S3] and 3) VN:α-syn + VC:α-syn: VN (1-158)-IDGGGGSGGGGSLK-α-syn + VC (159-239)-IDGGGGSGGGGSLK-α-syn. The VN:TsixK-α-syn and TsixK-α-syn:VC were generated by replacing the WT-α-syn in the VN: α-syn and α-syn:VC with TsixK-α-syn. Constructs obtained from other laboratories are noted in acknowledgements. All constructs were verified by sequencing. A guinea-pig polyclonal antibody was used for immunostaining total (mouse + human) α-syn [S4, S5]. Antibodies used for immunoblotting were: BD-α-syn (Clone 42/a-syn, BD-Transduction Lab., 610786), 2F12 [S1], anti-GFP (polyclonal, Abcam, ab290), anti-tubulin (Clone DM1A, Sigma, 9026). All chemicals were from Sigma unless specified otherwise.

Hippocampal Cultures, transfection and viral transduction

Primary hippocampal cultures were obtained from P0-P1 mouse pups and transiently transfected with Lipofectamine 2000 (Invitrogen) as described previously [S5, S6]. All animal studies were performed in accordance with University of California guidelines. For vGLUT1-pHluorin and synaptic-vesicle dispersion experiments, neurons were electroporated with the respective constructs before plating using an Amaxa 4D-Nucleofector™ System (Lonza Inc., Walkersville, MD) with the P3 Primary Cell 4D-Nucleofector X Kit S (V4XP-3032) and program CL-133. The volume of the cell suspension was 20 µl per reaction and the cell density ranged from 1×10^7 to 1.5×10^7 cells/ml. Cells were plated at a density of 60,000 cells/cm^2 onto poly-D-lysine coated coverslips after electroporation and cultured to maturity (DIV14-DIV21) before imaging. For transduction of adeno-associated virus (AAV) constructs, cultured DIV-7 neurons (60,000 cells/cm^2) were transduced with AAV-VN: α-syn ($1.49\text{x}10^{13}$) and AAV-α-syn:VC ($1.94\text{x}10^{13}$) at multiplicity of infection (MOI) equals to $1.5\text{x}10^5$. The vast majority of neurons were infected after 7 days, when lysates were collected for biochemistry.

Native PAGE gels

Native-PAGE was performed using standard protocols. All steps were carried out on ice and detergent free environment to keep the native interactions intact. Briefly, neurons and HEK293 cells expressing VN/VC: α-syn were lysed in buffer containing 50 mM NaCl, 50 mM Tris-Cl, 5 mM EDTA, pH 8.0 and protease inhibitors. After 12000 xg centrifugation, the supernatant was collected and quantified using BCA kit. 20 µg of total protein was resolved on Bis-Tris native-PAGE (Invitrogen). After transferring, PVDF membranes were fixed in PFA [S7] followed by Western blot analysis.

Recombinant expression, chemical crosslinking and purification of human synuclein

Human WT and TsixK mutant synucleins were cloned in pET28b+ vector and expressed in *E. coli* BL21(DE3) using 1 mM IPTG. For crosslinking, 1 mM DSG was added to the cell suspension in PBS with protease inhibitors before lysis for 1 h at 37 °C. Protein purification was performed according to standard protocols using ammonium sulfate precipitation followed by Q-Sepharose anion exchange chromatography. Desalted purified monomers and the mutimers were used for various biochemical analyses.

HEK293T Cultures and Transfections

HEK293T cells (ATCC) were maintained in DMEM medium (Invitrogen) containing 10% FBS (Thermo Scientific, San Diego, CA) and passaged every 3-4 days. Cells were transfected with DNA of interest by electroporation using Amaxa 4D system with SF Cell Line 4D-Nucleofector X Kit L (V4XC-2024) and program CM-130. The volume of the cell suspension was 100µl per reaction and the cell density ranged from 1×10^7 to 3×10^7 cells/ml. Cells were cultured for 24 hours post transfection and cell lysates were used for Native-PAGE analysis.

Microscopy, live cell Imaging and immunofluorescence

For synaptic targeting experiments (figs. 1 and 2), neurons were imaged live (maintained at 37°C) on an inverted motorized epifluorescence microscope (Olympus, IX81) fitted with a CoolSNAP HQ^2 camera [S6]. The filter sets used for YFP and RFP imaging were set 49003 and 42005 (Chroma). The excitation wavelength maximums (Emax) were 535 nm for YFP (520-550 nm) and 600 nm for RFP (570-626 nm) respectively; and there was no spectral overlap in our imaging conditions (data not shown). Z-stack images were obtained as previously described [S5] and all images were acquired and processed with MetaMorph software and MATLAB as noted in the text. The synaptic-vesicle dispersion assay and the pHluorin assays were done at room temperature on an inverted motorized epifluorescence microscope (Nikon, Ti Eclipse, Garden City, NY) fitted with an exquisitely-sensitive QuantEM 512SC EMCCD camera (Photometrics, Tucson, AZ) and LED excitation (Lumencor LED, Spectra X). For the vGLUT1-pHluorin experiments, coverslips with cultured neurons were mounted into a Chamlide EC magnetic chamber (Live cell Instrument, ON, Canada), and the entire system was perfused with Tyrode solution (pH 7.4) containing (in mM): 119 NaCl, 2.5 KCl, 2 $CaCl_2$, 2 $MgCl_2$, 25 HEPES, 30 glucose, 10 µM 6-cyano-7-nitroquinoxaline-2,3-dione (CNQX, TOCRIS bioscience, Bristol, UK), and 50 µM D,L-2-amino-5-phosphonovaleric acid (AP5, TOCRIS bioscience). For field-stimulation, 10 V pulses were applied at 10 H_Z for 60 seconds using an SD9-square-pulse stimulator (Grass Instruments, Middleton, WI). Incident excitation (Lumencor LED, Spectra X) was attenuated 10-fold and images were acquired with 500 ms exposures at either three second intervals for three minutes (vGLUT1-pHluorin) or six second intervals for 84 seconds (vesicle-dispersion assay).

Image Analysis

Synaptic co-localization algorithms: Registered Z-stack images were deconvolved (Huygens), max-projected and aligned as described previously [S5]. Regions of interest (ROIs) were placed around each bouton puncta, and further analyses were done in MATLAB. The puncta were then digitally-rotated around the weighted centroid at 20 discrete intervals of theta = 2π/20 (rad), and linear fluorescence projections were taken at each interval-angle. The mean of the 20 resulting line scans was approximated with a first order Gaussian, and the full-width half-max (FWHM) was calculated as $|2\sigma|\sqrt{\log(4)}$, where σ is the standard deviation of the Gaussian function (also see Supp. fig. 2B). FWHM is a quantitative measure of synapse-widths in our experiments [S8]. Illustrated by the figure on right, it is the width of the shaded region between points in an intensity-curve where the amplitude has dropped to half (1/2 * Fmax).

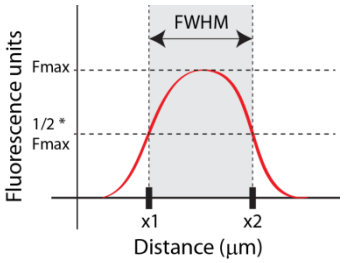

Quantification of vGLUT1-pHluorin and synaptic-vesicle dispersion assays. ROIs were placed on each bouton and average intensities were obtained for each frame within the time lapse. For vGLUT1-pHluorin experiments, F_{max} was defined as the average fluorescence of the maximal five frames after NH_4Cl perfusion. Baseline F_0 was defined as the average fluorescence of the initial 10 frames before stimulation [(F_0 = average (F_1:F_{10})]. Fluorescence intensity of a bouton at a given time point (F) was normalized to F_0 and F_{max} and expressed as $(F-F_0)/(F_{max}-F_0)$. For dispersion assays, fluorescence of a bouton at a given time point (F) was normalized to the average fluorescence of the initial five frames [(F_0 = average (F_1:F_5)] and expressed as F/F_0. Percentage of dispersion was expressed as $(F_{max} - F_{min})/F_0$ for each bouton.

Quantification of synaptic targeting factor. Targeting factor was calculated as described previously [S9], with some modifications. Briefly, the VN/VC-tagged protein of interest and soluble DsRed were co-transfected and fluorescence intensities were measured along lines drawn perpendicularly to the axons and across the boutons. Peak fluorescence along boutons and the adjacent axon were determined by fitting Gaussian functions to the resultant intensity profiles and corrected for background. Targeting factor was expressed as $(Bouton_{Green}/Axon_{Green})/(Bouton_{Red}/Axon_{Red}) - 1$.

In-vitro synaptic vesicle binding assay

Synaptic vesicle and cytosol from alpha-synuclein null mice cortices were isolated according to [S10]. Briefly, brain cortices were homogenized in buffer A (320 mM sucrose, 1 mM EGTA, 5 mM HEPES, pH 7.4) with protease inhibitors. After sequential centrifugation at 1000 xg and 13,300 xg for 10 min, crude synaptosomes were loaded onto a 5%-9%-13% Ficoll gradient prepared in buffer A and centrifuged at 35,000 xg for 35 min. Interface between 9%-13% was washed with buffer B (140 mM NaCl, 5 mM KCl, 20 mM HEPES, 5 mM $NaHCO_3$, 1.2 mM Na_2HPO_4, 1 mM $MgCl_2$, 10 mM glucose). Resultant pellet was incubated on ice for 10 min in buffer C (10 mM HEPES, 18 mM KOAc, pH 7.2) and centrifuged at 24000 xg to pellet down the

synaptic vesicles. Vesicle pellet was washed with buffer D (25 mM HEPES, 125 mM KOAc, 2.5 mM $MgCl_2$) and stored at -80°C till use. To isolate cytosol, cortices were processed in buffer containing 85 mM sucrose, 100 mM KOAc, 1 mM MgOAc and 20 mM HEPES, pH 7.4 and subjected to sequential centrifugation at 15, 000 xg and 100,000 xg. Resultant cytosol was dialyzed in buffer containing 145 mM KOAc and 25 mM HEPES, pH 7.2 and used for the vesicle binding assay. 30 µg purified protein was incubated with purified synaptic vesicles and KO-cytosol for 30 min at 37°C. Content was centrifuged at 24,000 xg for 10 min to separate bound and unbound fractions. After two rinses with buffer D samples were used for gel analysis and western blot.

Statistical Analysis

Statistical analyses were performed using Prism software (GraphPad, La Jolla, CA). Nonparametric Student's t-test was used for comparing two groups, and one-way ANOVA for multiple groups. Results are expressed as mean±SEM. A p value <0.05 was considered significant.

Supplementary References

S1. Dettmer, U., Newman, A.J., Luth, E.S., Bartels, T., and Selkoe, D. (2013). In vivo cross-linking reveals principally oligomeric forms of alpha-synuclein and beta-synuclein in neurons and non-neural cells. J Biol Chem *288*, 6371-6385.

S2. Outeiro, T.F., Putcha, P., Tetzlaff, J.E., Spoelgen, R., Koker, M., Carvalho, F., Hyman, B.T., and McLean, P.J. (2008). Formation of toxic oligomeric alpha-synuclein species in living cells. PLoS One *3*, e1867.

S3. So, P.P., Khodr, C.E., Chen, C.D., and Abraham, C.R. (2013). Comparable dimerization found in wildtype and familial Alzheimer's disease amyloid precursor protein mutants. Am J Neurodegener Dis *2*, 15-28.

S4. Scott, D.A., Tabarean, I., Tang, Y., Cartier, A., Masliah, E., and Roy, S. (2010). A pathologic cascade leading to synaptic dysfunction in alpha-synuclein-induced neurodegeneration. J Neurosci *30*, 8083-8095.

S5. Scott, D., and Roy, S. (2012). alpha-Synuclein inhibits intersynaptic vesicle mobility and maintains recycling-pool homeostasis. J Neurosci *32*, 10129-10135.

S6. Roy, S., Yang, G., Tang, Y., and Scott, D.A. (2011). A simple photoactivation and image analysis module for visualizing and analyzing axonal transport with high temporal resolution. Nat Protoc *7*, 62-68.

S7. Lee, B.R., and Kamitani, T. (2011). Improved immunodetection of endogenous alpha-synuclein. PLoS One *6*, e23939.

S8. Orenbuch, A., Shalev, L., Marra, V., Sinai, I., Lavy, Y., Kahn, J., Burden, J.J., Staras, K., and Gitler, D. (2012). Synapsin selectively controls the mobility of resting pool vesicles at hippocampal terminals. J Neurosci *32*, 3969-3980.

S9. Gitler, D., Xu, Y., Kao, H.T., Lin, D., Lim, S., Feng, J., Greengard, P., and Augustine, G.J. (2004). Molecular determinants of synapsin targeting to presynaptic terminals. J.Neurosci. *24*, 3711-3720.

S10. Wislet-Gendebien, S., Visanji, N.P., Whitehead, S.N., Marsilio, D., Hou, W., Figeys, D., Fraser, P.E., Bennett, S.A., and Tandon, A. (2008). Differential regulation of wild-type and mutant alpha-synuclein binding to synaptic membranes by cytosolic factors. BMC Neurosci *9*, 92.